NANO LETTERS

2009
Vol. 9, No. 7
2648-2653

Direct-Bandgap InAs Quantum-Dots Have Long-Range Electron−Hole Exchange whereas Indirect Gap Si Dots Have Short-Range Exchange

Jun-Wei Luo, Alberto Franceschetti, and Alex Zunger*

National Renewable Energy Laboratory, Golden, Colorado 80401

Received March 30, 2009; Revised Manuscript Received May 27, 2009

ABSTRACT

Excitons in quantum dots manifest a lower-energy spin-forbidden "dark" state below a spin-allowed "bright" state; this splitting originates from electron−hole (e-h) exchange interactions, which are strongly enhanced by quantum confinement. The e-h exchange interaction may have both a short-range and a long-range component. Calculating numerically the e-h exchange energies from atomistic pseudopotential wave functions, we show here that in direct-gap quantum dots (such as InAs) the e-h exchange interaction is dominated by the long-range component, whereas in indirect-gap quantum dots (such as Si) only the short-range component survives. As a result, the exciton dark/bright splitting scales as $1/R^2$ in InAs dots and $1/R^3$ in Si dots, where R is the quantum-dot radius.

One of the reasons for theoretical interest in semiconductor quantum dots is that the highly confined space in which electron and hole wave functions coexist enhances their overlap, thereby offering an interesting laboratory system for studying quantum confinement. Among the most notable effects caused by many-body interactions are the large exciton binding energy Δ_{coul} and dark/bright exciton exchange splitting Δ_X. The exciton binding energy Δ_{coul} is the energy difference between the lowest-energy exciton state and the single-particle gap ε_{gap}. Whereas in the one-band effective mass approximation Δ_{coul} has a characteristic $1/R$ dependence on the dot radius R,[1] it is now recognized that the size-scaling exponent ($\Delta_{coul} \propto R^{-\lambda_{coul}}$) is not universal and depends on the magnitude of the confining barrier and the extent of multiband coupling. Indeed, previous atomistic pseudopotential calculations[2−7] have found that $\lambda_{coul} \approx 1.2 - 1.4$ (which in some cases may be larger than the band-gap scaling exponent $\lambda_{gap} \approx 1.1 - 1.5$). The dark-bright exciton splitting Δ_X is the energy difference between the lowest energy spin-allowed ("bright") and spin-forbidden ("dark") exciton levels and is determined by electron−hole (e-h) exchange interactions. In general, the e-h exchange interaction can have a short-range (SR) and a long-range (LR) component.[8] In Table 1, we survey the literature on e-h exchange interactions in direct and indirect band gap semiconductors, including three-dimensional (3D) bulk, 2D quantum wells, and 0D quantum dots. In direct band gap *bulk* semiconductors, the SR exchange interaction is nonzero[9−11] and is responsible for the dark/bright exciton splitting. The LR exchange interaction is a dipole−dipole interaction,[9−11] which does not contribute to Δ_X but splits the bright excitons into a longitudinal and a transverse component.[9,12] For indirect bandgap bulk semiconductors, Bir and Pikus[10] found that the LR dipole−dipole component vanishes. In direct band gap 2D quantum wells,[13] the exchange interaction has both a SR and a LR component. The LR component is again dipole−dipole and vanishes linearly for exciton wavevector $Q_{\|} \rightarrow 0$. To our knowledge, there is no literature on the exchange interaction in indirect band gap quantum wells. For 0D spherical quantum dots, Efros et al.[14] and Takagahara[15] found, using the effective mass approximation, that only the SR exchange interaction contributes to the exciton splitting of direct and indirect excitons, while the LR component is zero. This is incorrect. Atomistic pseudopotential calculations[8] have shown instead that there is both a SR and a LR contribution to Δ_X in direct band gap quantum dots, whereas there is only a SR contribution in indirect band gap quantum dots. The previously overlooked LR component is a monopole–monopole interaction. This result was later confirmed by tight-binding calculations.[16] Little is known, however, on the underlying physics controlling the dependence of Δ_X on the dot radius ($\Delta_X \propto R^{-\lambda_X}$). The experimentally measured value of λ_X for InP[3] and InAs[17] quantum dots is ∼2, in contrast to $\lambda_X \sim 3$ for highly porous silicon.[18] In this paper, we will systematically study the exchange splitting Δ_X in direct bandgap InAs

* To whom correspondence should be addressed. E-mail: alex_zunger@nrel.gov.

10.1021/nl901000x CCC: $40.75
Published on Web 06/15/2009

Table 1. Survey of the Literature on SR and LR Exchange Interaction of Bulk, Quantum Wells, and Quantum Dots, Respectively (Present Results Shown in Boldface)

system (direct/indirect)		LR dipole−dipole	LR monopole−monopole	SR (analytic part)
3D-bulk	dir	nonzero[a,b]		nonzero[a,b]
	ind	zero[b]		nonzero[b]
2D-QW	dir	zero for $Q_{\|\|}\to 0$[c]		nonzero[c]
	ind	unknown		unknown
0D-QD	dir	zero[d] (incorrect); 10−20%[e]	**nonzero**[e,f]	**nonzero**[d,e,f]
	ind	zero[d,e,f]	**zero**[e,f]	**nonzero**[d,e,f]

[a] References 9 and 11. [b] Reference 10. [c] Reference 13. [d] References 14 and 15. [e] Reference 8. [f] Present paper.

and indirect bandgap Si quantum dots and explain how the balance between LR and SR exchange interactions affects the size dependence of Δ_X.

In standard model-Hamiltonian approaches based on the effective-mass approximation (EMA)[14] the e-h exchange interaction is described by a SR phenomenological Hamiltonian acting on the exciton envelope function

$$H_{\text{exch}}^{\text{EMA}} = -A_{\text{SR}}(\sigma \cdot J) \tag{1}$$

where

$$A_{\text{SR}} = \frac{2}{\pi}\xi\Delta_X^{(\text{b})}\left(\frac{a_0}{R}\right)^3 \tag{2}$$

ξ is a structure-dependent parameter defined in ref 14, and σ and J are the electron and hole spin operators, respectively. In this type of approach, the nature of the semiconductor material enters only via the bulk lattice constant a_0 and the bulk exchange splitting $\Delta_X^{(\text{b})}$. The LR e-h exchange interaction is an add-on to the theory and does not emerge from its structure. For example, Goupalov and Ivchenko[19] introduced an additional term

$$A_{\text{LR}} = \frac{\pi}{9}\chi\hbar\omega_{\text{LT}}\left(\frac{a_{\text{B}}}{R}\right)^3 \tag{3}$$

where χ is another structural parameter defined in ref 19, $\hbar\omega_{\text{LT}}$ is the longitudinal-transverse splitting of the bulk exciton, and a_{B} is the Bohr radius in the corresponding bulk semiconductor. While this model was determined to be consistent with earlier experimental observations[20,21] of $\Delta_X \sim R^{-3}$ in CdSe dots, recent experiments[22] found $\Delta_X \sim R^{-2}$. Similarly, the experimentally observed bright-dark splitting of InP and InAs quantum dots scales as $\sim R^{-2}$ (refs 3, 17).

Instead of introducing "by hand" the expressions of the LR and SR exchange as in eqs 1–3, here we construct an electronic structure theory where the size dependence of the e-h exchange interactions is an emerging phenomenon. The main quantity identifying the quantum-dot electronic structure is the single-particle potential $\hat{V}_{\text{dot}}$, taken as a superposition of overlapping, spherical potentials $v_\alpha(\mathbf{r})$ centered at the atomic positions $\{\mathbf{R}_{n,\alpha}\}$

$$\hat{V}_{\text{dot}} = \sum_\alpha \sum_n v_\alpha(\mathbf{r} - \mathbf{R}_{n,\alpha}) + \hat{V}_{\text{SO}} \tag{4}$$

The sum extends over the atoms in the quantum dot and the barrier material. The symmetry is built into $\{\mathbf{R}_{n,\alpha}\}$. Both the atomic potentials $\{v_\alpha\}$ and the spin−orbit operator $\hat{V}_{\text{SO}}$ are adjusted[23,24] to correctly reproduce bulk properties (i.e., when $\mathbf{R}_{n,\alpha}$ are bulk-periodic coordinates) such as effective masses, critical transition energies, deformation potentials, and spin−orbit splittings. Once $\hat{V}_{\text{dot}}$ is constructed for a given dot size, composition, and barrier material, the Schrödinger equation $[-(1/2)\nabla^2 + \hat{V}_{\text{dot}}]\psi_i = \varepsilon_i\psi_i$ is solved in a plane-wave basis set by direct diagonalization, producing the quantum-dot single-particle energies ε_i and wave functions $\{\psi_i\}$. The many-body exciton problem is set up as a configuration-interaction (CI) expansion[25]

$$\langle\Phi_{vc}|H|\Phi_{v'c'}\rangle = (\varepsilon_c - \varepsilon_v)\delta_{v,v'}\delta_{c,c'} - J_{vc,v'c'} + K_{vc,v'c'} \tag{5}$$

where J and K are the Coulomb and exchange integrals

$$J_{vc,v'c'}(S) = \sum_{\sigma_1,\sigma_2}\iint \frac{\psi_{v'}^*(\mathbf{r}_1,\sigma_1)\psi_c^*(\mathbf{r}_2,\sigma_2)\psi_v(\mathbf{r}_1,\sigma_1)\psi_{c'}(\mathbf{r}_2,\sigma_2)}{\bar{\varepsilon}(\mathbf{r}_1,\mathbf{r}_2)|\mathbf{r}_1 - \mathbf{r}_2|} \times \theta(S - |\mathbf{r}_1 - \mathbf{r}_2|)\mathrm{d}\mathbf{r}_1\mathrm{d}\mathbf{r}_2 \tag{6}$$

$$K_{vc,v'c'}(S) = \sum_{\sigma_1,\sigma_2}\iint \frac{\psi_{v'}^*(\mathbf{r}_1,\sigma_1)\psi_c^*(\mathbf{r}_2,\sigma_2)\psi_{c'}(\mathbf{r}_1,\sigma_1)\psi_v(\mathbf{r}_2,\sigma_2)}{\bar{\varepsilon}(\mathbf{r}_1,\mathbf{r}_2)|\mathbf{r}_1 - \mathbf{r}_2|} \times \theta(S - |\mathbf{r}_1 - \mathbf{r}_2|)\mathrm{d}\mathbf{r}_1\mathrm{d}\mathbf{r}_2 \tag{7}$$

The screening of the e-h interaction is described phenomenologically by the microscopic, position-dependent and size-dependent screening function $\bar{\varepsilon}(\mathbf{r},\mathbf{r}')$.[25] For reasons that will be explained later, we write both J and K as a function of the interaction radius S (ref 8) via a step function $\theta(S - |\mathbf{r}_1 - \mathbf{r}_2|)$ [$\theta(x) = 1$ for $x \geq 0$, otherwise $\theta(x) = 0$]. In our normal CI calculations, S is set to ∞. However, finite values of S will prove instructive later for analyzing the final results.

Spherical InAs quantum dots retain the T_d symmetry of the underlying bulk. Thus, the highest occupied molecular orbital (HOMO) and the lowest unoccupied molecular orbital (LUMO) of direct-gap InAs quantum dots have the Γ_8 and Γ_6 symmetry (in double group notation[26]), respectively. Spherical Si quantum dots embedded in a wide gap matrix have the O_h symmetry of the underlying bulk. Without considering spin−orbit interaction, the dot HOMO can be t_2 or t_1 and the dot

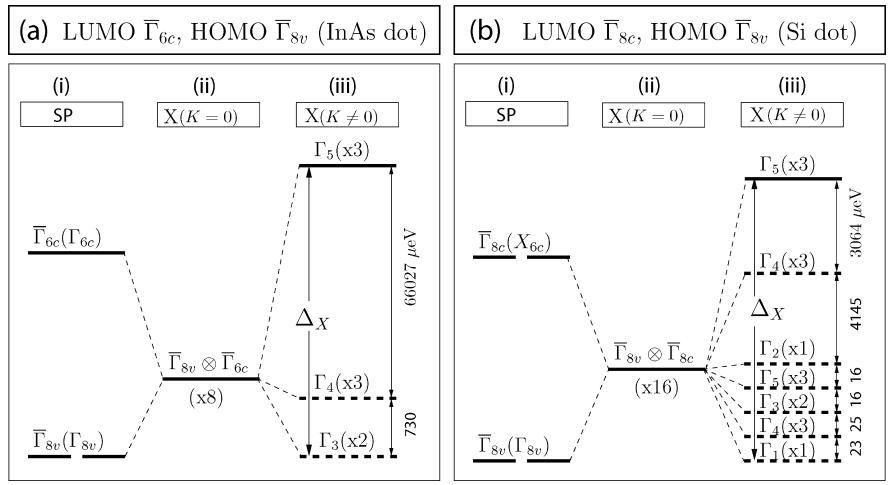

Figure 1. Evolution of exciton states from the single particle LUMO and HOMO states for (a) a spherical InAs dot of radius $R = 15$ Å and (b) a spherical Si dot of radius $R = 15$ Å. Single-particle states [column (i)] combine to produce an exciton state due to direct e-h Coulomb interaction, while neglecting all the e-h exchange interactions [column (ii)]. Column (iii) shows how the calculated level splittings due to the inclusion of all e-h Coulomb and exchange integrals. The e-h exchange induced exciton splittings are given in μeV.

LUMO can be a_1, e, or t_2 depending on the size of the dot.[2] The spin−orbit interaction splits t_2 into $\Gamma_8 + \Gamma_7$, t_1 into $\Gamma_8 + \Gamma_6$, and transforms e into Γ_8 and a_1 into Γ_6.[26] The calculated energy level diagrams (including spin−orbit interaction) are shown in Figure 1 column (i) for two cases: (a) InAs direct-gap quantum dots where the dot HOMO has the $\bar{\Gamma}_{8v}(\Gamma_{8v})$ symmetry and the LUMO has the $\bar{\Gamma}_{6c}(\Gamma_{6c})$ symmetry, leading to $\Gamma_8 \otimes \Gamma_6 = \Gamma_3 + \Gamma_4 + \Gamma_5$ excitons. (b) Si indirect-gap quantum dots with $\bar{\Gamma}_{8v}(\Gamma_{8v})$ HOMO and $\bar{\Gamma}_{8c}(X_{6c})$ LUMO (in our calculations the $\bar{\Gamma}_{8c}$ state is always below the $\bar{\Gamma}_{6c}$ state), leading to $\Gamma_8 \otimes \Gamma_8 = \Gamma_1 + \Gamma_2 + \Gamma_3 + 2\Gamma_4 + 2\Gamma_5$ excitons. Here the label in parentheses is the bulk state that folds into the dot state indicated by an overbar. Column (ii) in Figure 1 shows how the HOMO and LUMO single-particle states produce an exciton state due to direct e-h Coulomb interaction, but neglecting as yet all e-h exchange interactions. Column (iii) shows how the levels split due to the inclusion of all e-h Coulomb and exchange integrals. We define Δ_X as the energy separation between the lowest dark CI state (dotted line) and lowest bright CI state (solid line). The dark/bright character of the exciton states is determined by their dipole matrix elements with respect to the ground state. Although the Γ_5 symmetry is optically allowed, we find that the lower-energy Γ_5 excitons of Si dots have oscillator strength 3 orders of magnitude smaller than that of the higher-energy Γ_5 excitons, so we determine that only the higher-energy 3-fold Γ_5 excitons are bright.

To examine the magnitude of the SR and LR contributions, we calculate Δ_{coul} and Δ_X using the artificial step-function $\theta(S - |\mathbf{r}_1 - \mathbf{r}_2|)$ inserted in the integrals J [eq 6] and K [eq 7]. This step function truncates all contributions to the e-h Coulomb and exchange integrals when the electron and the hole are separated by a distance larger than S. Our results consist of plots of $\Delta_X(S)$ for different dot sizes. The asymptotic $S \rightarrow \infty$ limit gives the full dark/bright exchange splitting. Figure 2a shows $\Delta_X(S)$ for InAs quantum dots, whereas Figure 2b shows the ratio $\Delta_X(S)/\Delta_X(\infty)$. Figure 3

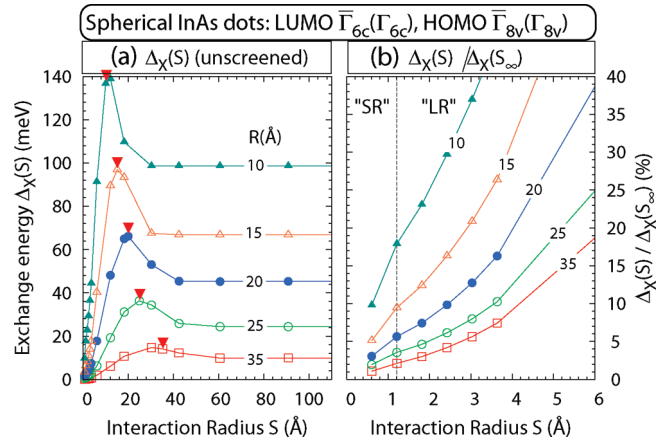

Figure 2. Unscreened ($\bar{\varepsilon} = 1$) exchange energy $\Delta_X(S)$ for direct-gap spherical InAs quantum dots. (a) The exchange energy $\Delta_X(S)$ is shown as a function of interaction radius S for different dot radii. The red triangles denote the dot radius R. (b) The plot of the percentage $\Delta_X(S)/\Delta_X$ ($S = \infty$) for dots of different sizes. The vertical dashed line indicates the Wigner−Seitz radius R_{WS}, which qualitatively separates the SR from the LR contributions to the exchange.

shows the same quantities for Si quantum dots. To determine the SR and LR contributions to Δ_X, we use as an arbitrary but useful demarcation point the Wigner−Seitz radius of the material, $R_{WS} = a_0(3/2\pi)^{1/3}/4$ (shown in Figures 2b and 3b as a vertical dashed line). We see from Figure 2 that in direct-gap spherical InAs quantum dots the exchange integrals have a significant LR contribution, originating from e-h separations larger than the Wigner−Seitz radius. In contrast, in indirect-gap spherical Si quantum dots [Figure 3] the dominant part of Δ_X is already established when the e-h separation is within the Wigner−Seitz radius, indicating that the e-h exchange interaction is almost entirely short ranged.

We find that the classification of LR-dominated exchange versus SR-dominated exchange correlates with the direct or indirect character of the single-particle HOMO−LUMO gap.

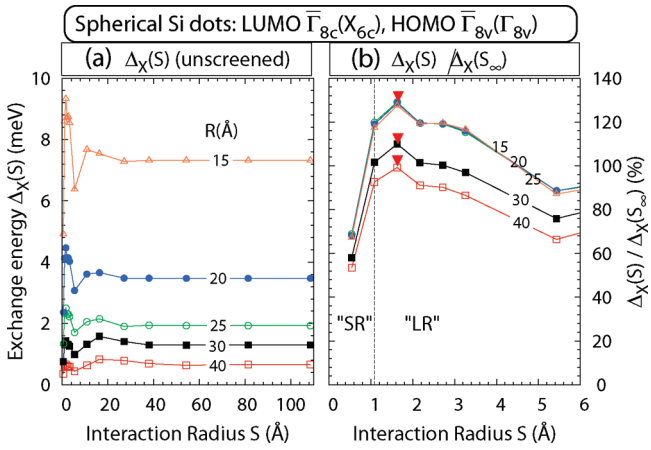

Figure 3. Same as Figure 2 but for indirect-gap spherical Si quantum dots. The red triangles denote the peak of $\Delta_X(S)$.

The origin of the HOMO and LUMO states can be determined by calculating the decomposition of the dot orbitals into bulk Bloch states throughout the Brillouin zone[27]

$$\psi_{(i)}^{dot}(\mathbf{r}) = \sum_{n,\mathbf{k}} C_{n,\mathbf{k}}^{(i)} u_{n,\mathbf{k}}(\mathbf{r}) e^{i\mathbf{k}\cdot\mathbf{r}} \tag{8}$$

Figure 4 shows this decomposition for spherical InAs and Si dots of radius $R = 15$ Å, clearly showing that the LUMO state of the InAs dot is a Γ-like state (98.2% derived from the bulk Bloch states around Γ), whereas the LUMO state of the Si dot is an *X*-like state (99.7% derived from the bulk Bloch states around *X*).

The correlation between the range of the exchange interaction and the direct/indirect character of the band gap can be understood based on the microscopic origin of the LR and SR exchange interactions. As shown in ref 8, the LR part of the e-h exchange interaction in quantum dots originates primarily from monopole−monopole interactions between transition charges located in each unit cell of the underlying bulk lattice. The exchange integral $K_{VC,VC}$ between the HOMO wave function (V) and the LUMO wave function (C) can be written as[8]

$$K_{VC,VC} = \sum_{m\neq n}^{N} \iint \frac{\chi_m^*(\mathbf{r}_1)\chi_n(\mathbf{r}_2)}{\bar{\varepsilon}(\mathbf{r}_1,\mathbf{r}_2)|\mathbf{r}_1 - \mathbf{r}_2|} d\mathbf{r}_1 d\mathbf{r}_2 \tag{9}$$

where

$$\chi_m(\mathbf{r}) = \sum_{\sigma} \psi_V(\mathbf{r},\sigma)\psi_C^*(\mathbf{r},\sigma) \tag{10}$$

if $\mathbf{r}$ is in the eight-atom unit cell Ω_m and 0 otherwise, and the sum runs over the primitive cells contained in the quantum dot. The LR monopole−monopole contribution to $K_{VC,VC}$ is

$$K_{VC,VC}^{M-M} = \sum_{m\neq n}^{N} \frac{q_m^* q_n}{\bar{\varepsilon}(\mathbf{R}_m - \mathbf{R}_n)|\mathbf{R}_m - \mathbf{R}_n|} \tag{11}$$

where $q_n = \int \chi_n(\mathbf{r}) d\mathbf{r}$ is the transition charge in the unit cell Ω_n located at $\mathbf{R}_n$. The monopole-monopole term exists because the electron and hole envelope functions are not constant inside each bulk-like unit cell. If they were, then $q_n \equiv 0$ (at least in the single-band effective mass approximation) because of the orthogonality of the bulk LUMO and HOMO Bloch functions. By Taylor expanding the hole and electron envelope functions in each unit cell n, we find that

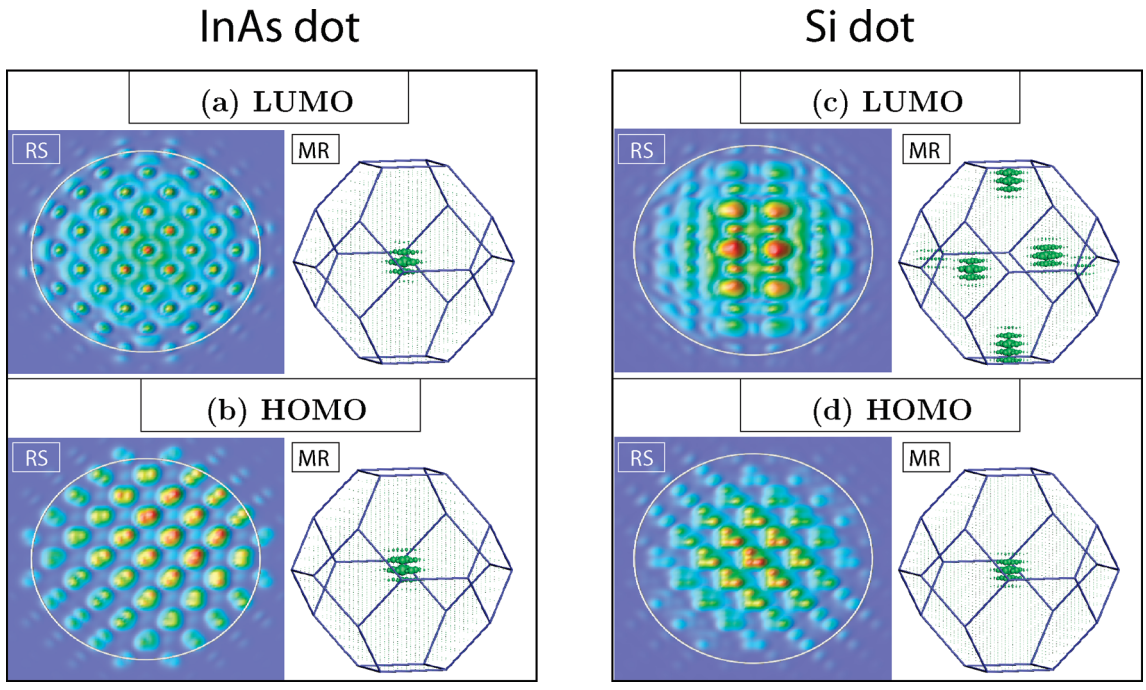

Figure 4. Real space (RS) wave function square and majority representation (MR) decomposition of single-particle (a) LUMO $\bar{\Gamma}_{6c}(\Gamma_{6c})$ and (b) HOMO $\bar{\Gamma}_{8v}(\Gamma_{8v})$ states for spherical InAs, and (c) LUMO $\bar{\Gamma}_{8c}(X_{6c})$ and (d) HOMO $\bar{\Gamma}_{8v}(\Gamma_{8v})$ states for spherical Si dot, respectively, with dot radius of $R = 15$ Å.

$$q_n \simeq \mathbf{r}_{V,C}[F_V(\mathbf{R}_n)\cdot\nabla F_C(\mathbf{R}_n) + F_C(\mathbf{R}_n)\cdot\nabla F_V(\mathbf{R}_n)] \quad (12)$$

where $F_{V,C}(\mathbf{R}_n)$ are the HOMO and LUMO envelope functions, respectively, and $\mathbf{r}_{V,C} = \langle\psi_V|\hat{\mathbf{r}}|\psi_C\rangle$ is the dipole matrix element between the bulk HOMO and LUMO Bloch functions. Thus, the lowest-order nonvanishing contribution to the transition charge q_n is proportional to the dipole matrix element $\mathbf{r}_{V,C}$. This implies that $q_n \neq 0$ in direct-gap semiconductors, and $q_n \sim 0$ (and therefore $\Delta_X^{LR} \sim 0$) in indirect-gap semiconductors.

Other important observations from Figures 2 and 3 and Table 2 are the following:

(i) The exciton binding energy Δ_{coul} is dominated by the LR direct Coulomb interaction. In the envelope-function approximation, assuming an infinite potential barrier at the surface of the quantum dot and a size-independent dielectric constant, one would expect $\lambda_{coul} \sim 1$. We find that in the absence of screening (i.e., for $\bar{\varepsilon} = 1$) $\lambda_{coul} = 0.87$ for InAs and $\lambda_{coul} = 0.80$ for Si, as shown in Table 2. The deviations from the $1/R$ scaling are due primarily to the electron and hole wave functions "spilling out" of the quantum dot as the size becomes smaller.[7] When screening is included ($\bar{\varepsilon} > 1$) Δ_{coul} decays more rapidly with size because the dielectric constant of the quantum dot decreases as the size decreases.[28] We find $\lambda_{coul} = 1.39$ for InAs quantum dots and $\lambda_{coul} = 1.22$ for Si quantum dots (see Table 2).

(ii) The exchange energy $\Delta_X(S)$ is a nonmonotonic function of S. For direct-gap InAs dots, $\Delta_X(S)$ has a pronounced peak for S equal to the dot radius R (red triangles in Figure 2a). In contrast, for indirect-gap Si dots $\Delta_X(S)$ has an oscillatory structure (Figure 3a) with its peak close to R_{WS} (red triangles in Figure 3b). We tentatively attribute the peak at $S = R$ for direct-gap InAs dots to the distortion of electron and hole wave functions at the dot-barrier interface.[29] Another evidence to support this assumption is that the distance between peak-to-plateau in Figure 2a increases as the dot size R decreases which has the same trend as the distortion of the electron and hole wave functions.

(iii) The size dependence of Δ_X depends on the balance between the LR contribution (scaling as $\sim 1/R$) and the SR contribution (scaling as $\sim 1/R^3$) and is further modified by dielectric screening, which affects the LR component much more than the SR component.[8] Figure 5 shows the dependence of Δ_X with and without screening on the quantum dot radius for InAs (Figure 5a) and Si (Figure 5b) quantum dots. From the size dependence of Δ_X, we extract the scaling exponent λ_X given in Table 2. In the case of InAs dots, we find that for $\bar{\varepsilon} = 1$ the SR part of Δ_X (Δ_X^{SR}) scales as $1/R^{2.55}$, whereas Δ_X^{LR} scales as $1/R^{1.25}$. Including both SR and LR contributions, we obtain $\lambda_X = 1.79$ (without screening) and $\lambda_X = 2.21$ with screening. In the case of Si quantum dots, the LR component of Δ_X is negligible (see Figure 2), so the scaling of Δ_X is dominated by the SR part. We find $\lambda_X = 2.85$ without screening ($\bar{\varepsilon} = 1$) and $\lambda_X = 3.0$ when screening is included. Note that screening affects λ_X of InAs quantum dots more than Si quantum dots, because the LR exchange component (which is present in InAs but not in Si) is more sensitive to screening than the SR exchange component.

Table 2. The Size Scaling Exponent λ of the Single-Particle Band Gap ε_{gap}, the Direct Coulomb Energy Δ_{coul} (Screened and Unscreened), and the Exchange Energy Δ_X (Screened and Unscreened) for Spherical InAs and Si Quantum Dots[a]

	InAs dots (direct)		Si dots (indirect)	
energy	λ_{unscr}	λ_{scr}	λ_{unscr}	λ_{scr}
ε_{gap}	1.09		1.51	
Δ_{coul}	0.87	1.39	0.80	1.22
Δ_X^{SR}	2.55	2.91	2.34	2.72
Δ_X^{LR}	1.25	1.59	–	–
Δ_X	1.79	2.21	2.85	3.00

[a] The size scaling of the SR exchange component Δ_X^{SR} and LR exchange component Δ_X^{LR} is also given. Δ_{coul} and Δ_X are fitted to the expression a/R^{λ}.

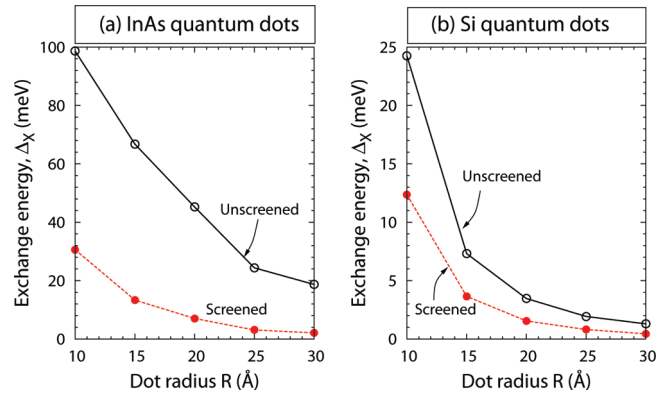

Figure 5. The unscreened (black solid lines) and screened (red dashed lines) exchange splittings are shown as a function of dot sizes for (a) spherical InAs quantum dots and (b) spherical Si quantum dots.

We conclude that the scaling of Δ_X with size depends sensitively on the relative magnitude of the SR and LR components of the exchange integrals. Direct-gap quantum dots, where the LR part is at least as large as the SR part, have $\lambda_X \sim 2$, whereas indirect-gap quantum dots, where the SR component is dominant, have $\lambda_X \sim 3$.

Acknowledgment. This work was funded by the U.S. Department of Energy, Office of Science, Basic Energy Science, Materials Sciences and Engineering Division, under Contract No. DE-AC36−08GO28308 to NREL.

References

(1) Harrison, P. *Quantum Wells, Wires and Dots: Theoretical and Computational Physics of Semiconductors Nanostructures*; Wiley, New York, 2000.
(2) Reboredo, F. A.; Franceschetti, A.; Zunger, A. *Phys. Rev. B* **2000**, *61*, 13073.
(3) Micic, O. I.; Cheong, H. M.; Fu, H.; Zunger, A.; Sprague, J. R.; Mascarenhas, A.; Nozik, A. J. *J. Phys. Chem. B* **1997**, *101*, 4904.
(4) Williamson, A. J.; Zunger, A. *Phys. Rev. B* **2000**, *61*, 1978.
(5) Fu, H.; Zunger, A. *Phys. Rev. B* **1997**, *55*, 1642.
(6) Wang, L. W.; Zunger, A. *J. Phys. Chem.* **1998**, *102*, 6449.
(7) Franceschetti, A.; Zunger, A. *Phys. Rev. Lett.* **1997**, *78*, 915.
(8) Franceschetti, A.; Wang, L. W.; Fu, H.; Zunger, A. *Phys. Rev. B* **1998**, *58*, R13367.
(9) Rössler, U.; Trebin, H. R. *Phys. Rev. B* **1981**, *23*, 1961.
(10) Bir, G. L. Pikus, G. E. *Symmetry and strain-induced effects in semiconductors*; Wiley, New York, 1974.
(11) Cho, K. *Phys. Rev. B* **1976**, *14*, 4463.
(12) Suffczyński, M.; Swierkowski, L.; Wardzyński, W. *J. Phys. C: Solid State Phys.* **1975**, *8*, L52.

(13) Jorda, S.; Rössler, U.; Broido, D. *Phys. Rev. B* **1993**, *48*, 1669.
(14) Efros, Al. L.; Rosen, M.; Kuno, M.; Nirmal, M.; Norris, D. J.; Bawendi, M. *Phys. Rev. B* **1996**, *54*, 4843.
(15) Takagahara, T. *Phys. Rev. B* **1993**, *47*, 4569.
(16) Lee, S.; Jönsson, L.; Wilkins, J. W.; Bryant, G. W.; Klimeck, G. *Phys. Rev. B* **2001**, *63*, 195318.
(17) Banin, U.; Lee, J. C.; Guzelian, A. A.; Kadavanich, A. V.; Alivisatos, A. P. *Superlattices Microstruct.* **1997**, *22*, 559.
(18) Calcott, P. D.; Nash, K. J.; Canham, L. T.; Kane, M. J.; Brumhead, D. *J. Phys.: Condens. Matter* **1993**, *5*, L91.
(19) Goupalov, S. V.; Ivchenko, E. L. *Fiz. Tverd. Tela (Leningrad)* **2000**, *42*, 1976; see also *Phys. Solid State* **2000**, *42*, 2030.
(20) Norris, D. J.; Efros, Al. L.; Rosen, M.; Bawendi, M. G. *Phys. Rev. B* **1996**, *53*, 16347.
(21) Chamarro, M.; Gourdon, C.; Lavallard, P.; Lublinskaya, O.; Ekimov, A. I. *Phys. Rev. B* **1996**, *53*, 1336.
(22) Liptay, T. J.; Marshall, L. F.; Rao, P. S.; Ram, R. J.; Bawendi, M. G. *Phys. Rev. B* **2007**, *76*, 155314.
(23) Wang, L. W.; Zunger, A. *Phys. Rev. B* **1995**, *51*, 17398.
(24) Wang, L. W.; Kim, J.; Zunger, A. *Phys. Rev. B* **1999**, *59*, 5678.
(25) Franceschetti, A.; Fu, H.; Wang, L. W.; Zunger, A. *Phys. Rev. B* **1999**, *60*, 1819.
(26) Dresselhaus, G. *Phys. Rev.* **1955**, *100*, 580.
(27) Wang, L. W.; Bellaiche, L.; Wei, S. H.; Zunger, A. *Phys. Rev. Lett.* **1998**, *80*, 4725.
(28) Wang, L. W.; Zunger, A. *Phys. Rev. Lett.* **1994**, *73*, 1039.
(29) Luo, J. W.; Li, S. S.; Xia, J. B.; Wang, L. W. *Appl. Phys. Lett.* **2006**, *88*, 143108.

NL901000X